The effects of test parameters on the impact response of glass reinforced plastic using an experimental design approach

L. S. Sutherland and C. Guedes Soares

Abstract

An instrumented falling weight machine was used to investigate the effects of test parameters on the impact response of low fibre-volume E-glass woven-roving reinforced polyester coupons. Statistical experimental design techniques were used to plan the experiment and to analyse the data. All the parameters considered were found to affect the responses in a complex and interacting manner. Multiple damage modes occurred and the damage mechanisms were seen to vary with the test parameters. Identification of the important parameter effects above the experimental variation using statistical methods combined with graphical representation of these effects and the failure modes simplified the interpretation of the results. It was demonstrated that the techniques of statistical design of experiments are powerful to identify the interaction among parameters that govern the structural response in particular when there are many parameters.

Keywords

Glass fibres (A); PMCs (A), Impact Behaviour (B); Experimental Design; Statistics (C).

1. Introduction

Laminated fibre reinforced plastic composite materials are now used extensively in many fields of engineering, but their susceptibility to impact damage is not well known. The fact that such damage may remain undetected and also be extended by repeated impacts or other cyclic loads further exacerbates the problem. These concerns have led to a great deal of research work investigating various areas of the problem using many different approaches. However, there is now a general consensus of opinion on the main features as described in the brief overview of the literature given below. For more detailed and complete information Abrate [1] provides an excellent classification of the different aspects of the field.

A huge proportion of the work carried out to date has been driven by the Aerospace industry with the associated high-cost, high fibre-volume, mostly carbon composites. Most of the work concerns unidirectional composites, although recent work has tackled the more complex behaviour of woven fabric laminates [2–4]. However, high-speed craft such as ferries and patrol craft are now an increasingly important part of the marine industry, and the use of lightweight, corrosion resistant, readily fabricated and formed composite materials is ideal for such applications. Composites are also the dominant material for pleasure boat construction and are extensively used in the construction of fishing vessels. There is currently little knowledge of the impact responses and mechanisms of the types of composites used in the marine industry (usually low-fibre fraction woven and discontinuous glass-fibre reinforced polyester), and design data is rare. The high variability of these hand-laminated materials adds to the interest of the already complex impact problem. Safety factors of up to 10 are applied when marine composite structures will be subjected to impact loads [5] obviously severely detracting from the attractiveness of their high specific

material properties. These types of low fibre-fraction materials are also commonly used in other fields such as the civil and chemical industries.

Typically examples of impact events relevant to marine craft are: tool drops and other construction accidents, repeated light docking collisions, and collisions with floating debris and other vessels. These types of impact may be categorised as low-velocity impacts and hence low-velocity impact is considered in this study. Here the effects of the propagation of stress waves through the material are negligible, the structure has time to respond to the impact and the response may approach that of the static case. In their review of low-velocity impact properties Richardson and Wisheart [6] note that there is conflicting information regarding the strain rate sensitivity of glass fibres. They write that the modulus of glass fibres is thought to increase with strain rate but they agree with the view of Sierakowski and Chaturvedi [7] that there is insufficient information to assess the role of the rate sensitivity of composite systems. However, quasi-static testing may often be used to give valuable damage and indentation data [8].

The behaviour of an impacted laminate is generally considered in two phases; the localised contact problem and the overall target deflection. Indentation at the surface may be modelled by a Hertzian contact law (e.g. [9,10]). The deformation of the target may be 'exactly' described by complete models using beam or plate theories (e.g. [11]). However, these models apply for simple cases for small deflections but are difficult to interpret and rapidly become too computationally expensive when considering more complex architectures or cases with significant shear deformations. They are also not effective for the consideration of damage. A more approximate and realistic approach in these latter cases is to use theories to describe the overall response of the composite. For example, the energy balance method assumes that when the maximum deflection is reached the projectile velocity is zero and all the incident energy has been used to deform and damage the structure [12,13]. Abrate [14] gives a comprehensive overview of all of the main modelling techniques used.

Impact damage consists of complex mixtures of delaminations, matrix cracking and damage, and fibre failure. Richardson and Wisheart [6] give an extensive description of the occurrences of each type of failure mode. Simple damage area models assume delamination at a radius from the impactor where the average interlaminar shear stress exceeds the corresponding shear strength [15,16]. Non-destructive damage evaluation methods used for opaque laminates include ultrasonic [17], X-ray and thermographic, but these methods are expensive and features may be obscured due to the non-homogenous nature of the material. Damage in translucent laminates may be simply viewed by strong backlighting [18,19].

The critical effect of the delamination of impact-damaged composites is the reduced compression strength, and compression after impact (CAI) tests are common (e.g. [20]). Caprino [21] developed a simple model based on linear elastic fracture mechanics to predict residual compressive strength.

However, despite the large amount of work in the area, the impact testing of composite materials has proved to be difficult to standardise. This is because the ostensibly simple impact event does in fact have many and complex dynamic consequences which are highly dependent on many and interacting material and test variables. When this impact event

concerns composite materials with their intricate microstructure and hence correspondingly complex responses and failures, the complexity of the problem is compounded. Christoforou [22] found that impact response varied according to both impactor and structure characteristics, influencing both the form and extent of the damage suffered. Caprino et al. [23] noted that, "…despite the availability of many studies published over the last two decades the wide range of specimen geometries and impactor parameters used render difficult a comparison of the experimental results and the assessment of general laws." This view is restated in Caprino and Lopresto [24], and in Cartié and Irving [25] a figure of 14 different parameters that are likely to influence the performance of a composite structure is quoted. In fact these latter two papers illustrate well the point that direct comparisons of different test set-ups and materials may lead to apparently contradictory conclusions. Caprino and Lopresto [24] conclude that the fibre volume is most important whereas resin type and content is secondary; Cartié and Irving [25] conclude that the influence of the fracture toughness of the resin is strong, whereas the fibre type did not improve the resistance to impact. Hirei et al. [26] and Kessler and Bledzki [27] found that the fibre surface treatment may be as important as the fibre and matrix materials used.

These problems of standardisation are directly linked to the problems of relating test data to the full-scale end use. Problems exist both in scaling laboratory coupon data to full-scale and in interpreting the results under test conditions in terms of in-service behaviour. Morton [28] used the Buckingham Pi method of dimensional analysis, and Swanson et al. [29] considered the governing equations of the system to develop scaling laws. However, the scaling of the damage area was not successful. Greenhalgh et al. [30] and Found et al. [31,32] investigated the response of stiffened panels (as a common example of a full-scale component) to impacts in different parts of the structure. Greenhalgh et al. [30] pessimistically concluded that, "The results of impact tests on plain laminates can not be extrapolated and applied directly to composite structures." They also note that both material and panel geometry parameters affected both the damage area and resistance.

The objective of this study is to empirically investigate the effects of some important test and material parameters on the low-velocity impact behaviour of marine composites. However, there are numerous variables to consider and, very importantly, following the discussion above, the effects of each of these parameters may well be themselves dependant on other variables. This interaction between variables would make the normal approach of a parametric study followed by simple inspection of the results prohibitively complex for any more than two or possibly three variables. Also, the variability of the materials studied may well make it difficult to distinguish parameter effects above the background experimental variation (or conversely, apparent effects may in fact be solely due to experimental variation).

The methodology of statistical experimental design has been developed to address such problems where multiple, interacting variables with significant experimental variation make interpretation of the data complex and difficult. Since, as described above, the impact problem for composite materials involves many interacting variables with considerable experimental scatter, this makes such techniques an ideal research tool here. This paper aims to use a simple case of experimental design to illustrate the general approach of the method. In fact, as will be seen, the design used corresponds to that of a full parametric study, but the analysis of the data follows the methodology of statistical experimental

design to ensure straightforward, methodical and efficient retrieval of all the available information above the background experimental variation.

An important ethos of the experimental design philosophy is that all experimentation should not be carried out in one stage. A cyclic approach is taken whereby an initial experiment is planned, executed and analysed and this data is used to plan the next phase of experimentation and so on. The initial or 'screening' study serves to identify the important variables and, most importantly, also the interactions between them. This gives an overview of the behaviour of the system and allows the efficient planning of a next stage of experimentation with the aim of investigating the effects of the pertinent variables in more detail. This study was conceived as such a screening study, to give a global view of the impact behaviour.

2. Statistical experimental design

Originally developed in the field of agricultural research [33], this large and well-established area has been very successfully applied in many other fields, especially product design, production engineering and quality control [34]. The technique may be split into two parts; the planning, or design, of the experiment, and then the statistical analysis of the results obtained. The experimental plan is specifically designed to ensure that the statistical analysis that will follow gives the maximum information for the minimum experimental resources.

As in most fields, statistical experimental design uses its own terminology to describe and define the problem and the important terms will first be explained. The design of the present experiment is then outlined, followed by a description of how the effects of each factor and their interactions may be simply and clearly presented using graphical methods. Next, for the simple case considered, the statistical approach used to decide which of these apparent effects are important, and which may only be attributable to experimental variation, or noise, is described. Finally an overview of the interpretation of the results of the analyses in terms of the physical system is given.

Only a very brief introduction to the statistical analysis of experimental design data may be given here, and it must be stressed that the example presented here constitutes only a simple case of experimental design. Further and more detailed information is widely available on the subject in the large amount of literature available (e.g. [35–37]).

2.1. Terminology

In this case a specific form of experimental design will be used known as ***factorial experimental design***. Here the experiment consists of a number of experimental ***runs*** where the experimental parameters or ***factors*** are varied between each ***run*** and the experimental ***response*** is measured in each case. The ***experimental design*** consists of a plan of the specific values, or ***levels*** of the factors to be used for each ***run***. ***Factor levels*** may be ***quantitative*** (e.g. Energy: 10J, 20J etc.) or ***qualitative*** (e.g. Shape: Square, Circular etc.), the interpretation of the latter type often requiring extra care. The objective of the experiment is to determine how changes in the values or levels of each factor change the response, and these effects are called ***factor effects***. An ***Interaction effect*** quantifies any differences between the effects of one factor at different values of another factor. Interactions are further described in Section 2.3.

The simplest factorial design, but also the one requiring the most experimental resources, is one in which all combinations of the factors levels are used and is termed a '***Full Factorial***'. '***Fractional Factorial***' designs, in which a carefully chosen, balanced subset of the possible runs is selected, can substantially reduce the number of experimental runs required to obtain the same amount of information. This is due to the way in which the statistical analysis uses all the experimental data to estimate the experimental variation. If it is known previously through a knowledge of the system that more complicated interactions between three or more factors are negligible, then calculated values of these effects may be used as an estimate of the experimental variation, without the need for run repetition or even the full set of factor level combinations [35,37–39].

The definition of an experiment as the determination of effects through measurement of the response for various experimental runs with the factors set at different levels is applicable to almost any scientific experiment. However, the main advantages of experimental design are that careful selection of the combination of runs and levels allows an efficient statistically based analysis of the data, and that each factor is not considered in turn and in isolation.

2.2. Experimental design

The first step is to decide which are the *responses* that should be measured and recorded in the experiments. For the impact problem the target deformation, the magnitudes of the resultant forces and the extent of any damage incurred are all of interest. The use of an instrumented falling weight machine and simple backlighting of damaged specimens (see Section 3) enables the measurement the following responses:

(i) Maximum central deflection of target.
(ii) Maximum force.
(iii) Energy irreversibly absorbed by specimen (related to damage incurred).
(iv) Projected delaminated damage area.

Previous experience of using experimental design methods for composite materials testing (Sutherland [40], Sutherland et al. [37–39] has shown that, since interaction between the parameters is common and often complex and that composite materials testing gives a high degree of experimental variability, the screening experiment design should be of a simple *Full Factorial* design, with only two levels taken by each factor in order to simplify both the statistical analysis and the subsequent interpretation of the results. Since it was possible to fabricate the specimens in-house relatively easily, it was decided to further increase the '***statistical resolution***' of the design by including three replications of each run.

The next step is to decide which *factors* should be investigated and at which *levels* they should be set. For drop-weight tests the specimen is supported and an impactor is dropped onto it in a controlled manner. The incident energy, incident velocity, impactor shape, and specimen geometry and support conditions may all affect the impact event. However, previous work suggested that any effects of impact velocity would not be distinguishable for the narrow range of velocities obtainable using the drop-weight test machine employed [18,19], and so this factor was not investigated here.

It is common practice with drop-weight tests to use a fully clamped plate target. The plate geometry may be circular (simplifying the analysis of the behaviour), or square (closer to

most real applications). Hence a 'Clamp' factor was designated with 'Rectangular' and 'Circular' as the two levels. Previous work [18,19] had also raised the possibility of unplanned specimen slippage at higher energies. The fact that the specimens had an irregular surface reduced the effective clamping area. In order to see if this had been influential by attempting to reduce any slippage, the two levels of a 'Grip' factor were defined as the presence of, and the absence of sandpaper grip on the faces of the clamps.

The two most common geometries for the impactor considered by the literature are hemispherical- and flat-ended cylinders. Thus these impactor shapes were set as the two levels of the factor 'Head'. Two levels of incident energy were selected, a 'low' energy level to correspond to the case where minimum delamination damage due to a modest impact event is desirable, and a 'high' energy level set closer to the perforation energy, where resistance to total perforation, energy absorption and ease of repair are more relevant.

A summary of the experimental design used is given in Table 1.

Run Nos.	**Energy**	**Clamp**	**Grip**	**Head**
1-3	Low	Circular	None	Flat
4-6	Low	Circular	None	Hemispherical
7-9	Low	Circular	Sandpaper	Flat
10-12	Low	Circular	Sandpaper	Hemispherical
13-15	Low	Rectangular	None	Flat
16-18	Low	Rectangular	None	Hemispherical
19-21	Low	Rectangular	Sandpaper	Flat
22-24	Low	Rectangular	Sandpaper	Hemispherical
25-27	High	Circular	None	Flat
28-30	High	Circular	None	Hemispherical
31-33	High	Circular	Sandpaper	Flat
34-36	High	Circular	Sandpaper	Hemispherical
37-39	High	Rectangular	None	Flat
40-42	High	Rectangular	None	Hemispherical
43-45	High	Rectangular	Sandpaper	Flat
46-48	High	Rectangular	Sandpaper	Hemispherical

Table 1. Full factorial experimental design

2.3. Graphical presentation of results

A simple and effective way in which to represent the effect of a factor is to plot the average response at both levels of the factor, as shown for a hypothetical factor 'A' in Fig. 1(a). The slope of the line represents what is called the '***factor main effect***'. This simple averaging process is valid despite the various other levels taken by the other factors because of what is termed the '***balance***' of the design. A full explanation of the term balance may be found in Grove and Davis [35] or Sutherland et al. [37], but in this case it means that, of the set of

runs averaged to give the response at a given level of any one factor, half will have any other given factor at the high level and half will have this other factor at the low level.

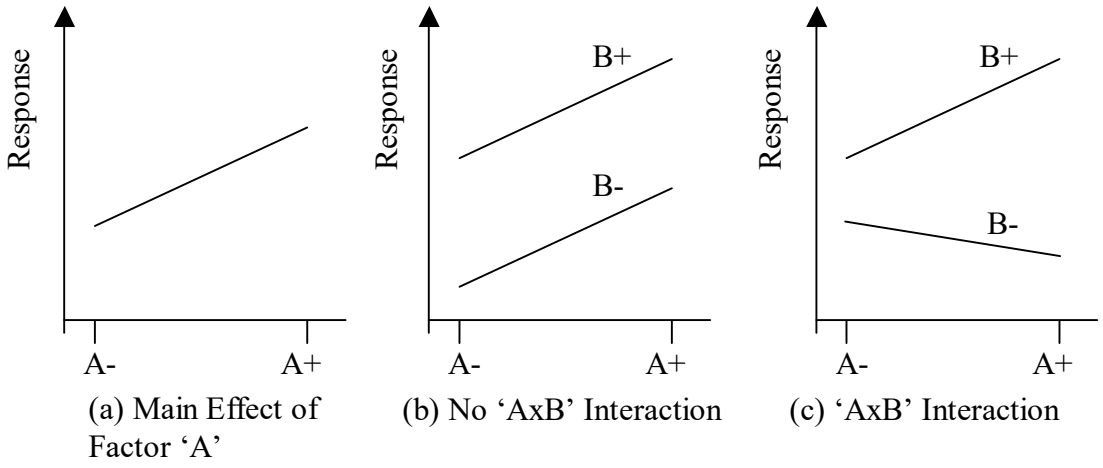

Fig. 1. Main and interaction effects.

Using this simple graphical approach it is now possible to define ***interaction effects*** between two factors. In Fig. 1(b) the effect of factor '*A*' is plotted for the two levels of a second factor '*B*'. In this case, although there is an effect of '*B*' (since the two lines are displaced from one another) the slopes and hence the effect of '*A*' are the same at both levels of '*B*'. In this case there is no interaction between '*A*' and '*B*'.

However in Fig. 1(c) a different case is presented where the slopes of the two lines are not equal. The effect of '*A*' is different at each of the different levels of '*B*' and there is said to be a '***two-way interaction***' between the two factors, denoted '*A*×*B*'. In this case the slopes have opposite signs, but interaction is present for any case where the two lines are not parallel. Furthermore, if (b) and (c) in Fig. 1 represented the '*A*' and '*B*' effects at the different levels of a third factor '*C*' then, since the behaviour is different in each plot, there is said to be a '***three-way interaction***' '*A*×*B*×*C*'. These definitions can be extended to ***four-way*** and other ***higher-order interactions***, but quickly become very difficult to interpret and to represent graphically.

It is important to realise that if there are important interactions then the main effects have little meaning in isolation. As an illustration consider the two-way interaction in Fig. 1(c) where the '*A*' effects are of opposite sign but of similar magnitude for the two levels of '*B*'. In this case the main effect of '*A*' will appear to be very small when averaged over the levels '*B*'. The incorrect conclusion that '*A*' has no bearing on the system will be made unless the interaction is taken into account. This point may be extended to include apparently non-significant two-way effects that form part of significant three-way interaction effects.

Another point that must be raised here is that for qualitative factors care must be taken with the interpretation of factor main effects. Again consider the illustrative example with two factors in Fig. 1, but in this case assume that '*B*' is qualitative with levels circular and rectangular (as for the 'Clamp' factor in this study). It is now important to be clear that the main effect of '*A*' will be that averaged over the two qualitative levels of '*B*', and that this raises the question of how this should be interpreted. There is no obvious clamp geometry halfway between rectangular and square, and hence the main effect of '*A*' is only of relevance if its interactions with '*B*' are insignificant as in Fig. 1(b). In this case '*A*' has the

same effect as both levels of '*B*' and so the 'average' value may be used to describe the behaviour at either level of '*B*'. In Fig. 1(c) this is not the case and the interactions must be considered, the main effect having little physical interpretation.

2.4. Statistical analysis of results

The testing of composite materials, especially of the type considered here, gives rise to data containing considerable experimental scatter. This makes it important to be able to distinguish if measured effects are 'real' (in statistical terms '*significant*') or are only apparent 'by chance' due to the experimental scatter present. With the simple experimental design used here the statistical techniques that may be used are correspondingly straightforward.

Statistical methods are used to fit a linear statistical model to the response data, with factor levels coded as −1 or +1 for each factor. A statistical model is specified, and the method calculates the coefficients of the main and interaction terms to give the 'best-fit' to the data by minimising the experimental error. The statistical methods available include ANOVA and multiple linear regression methods [36]. These methods may be easily completed with dedicated statistical software packages or for simple cases spreadsheets may be constructed [35].

Since a full factorial design with three repetitions of each run is used here, a *full model* containing all of the main and interaction effects may be used. An example of such a statistical model for a three factor experiment is given in Eq. (1).

$$y = k_1 A + k_2 B + k_3 C + k_4 AxB + k_5 AxC + k_6 BxC + k_7 AxBxC + \varepsilon \qquad (1)$$

where *A*, *B* and *C* are the coded factor levels, the *k*'s are coefficients and ε is the experimental error.

Usually, the coefficients are not written and Eq. (1) is simply expressed as:

$$y = A + B + C + AxB + AxC + BxC + AxBxC + \varepsilon \qquad (2)$$

Once the main and interaction effect coefficients have been calculated, an estimate of the experimental variation is made and each of these effects compared with this estimate in turn. By assuming that the experimental variation is normally distributed and does not vary between any of the factor levels, the probability that the effect is not 'real' and is in fact due only to experimental variation is calculated. These results are given as '*P*-values', and may be simply interpreted as a low *P*-value indicates that the effect is *significant* and should be taken into account. What is meant by a 'low' *P*-value depends on the severity of the consequences of making a false conclusion, but generally a value of 0.05 (i.e. 5%) is a good guideline for this type of experiment.

Before the *P*-values may be used with confidence, the assumptions about the experimental variability made by the statistical analysis must be verified in a *residual analysis* [36]. The success with which the model has been fitted to the data is given by the '*R*-Squared' value. A value of 100% means that all the data lies on the fitted line, a low value indicating that the

experimental scatter is high, or either that an inappropriate model has been fitted or that important terms have been omitted.

2.5. Interpretation of results

It is important to emphasise that in analysing the data the statistical analyses above are only a tool to aid the interpretation of the results. They should not be used in isolation with an indiscriminate cut-off at a *P*-value of 0.05, but must be used together with the existing knowledge of the physical system and the observed effects to explain the phenomena seen.

The approach taken can be described in three simple steps:

1. Main and interaction plots as described above are produced to simply and clearly summarise what may well be complex behaviour.
2. The important effects are identified above the background experimental variation (or 'noise') with a statistical analysis.
3. Knowledge of the physical system is used to interpret the important effects identified in step 2 using the plots produced in step 1.

It may well be that the screening experiment can only indicate the important areas of the behaviour, suggesting where more in-depth investigation is needed. The important point is that such an experiment gives a global view of the effects of each parameter on the behaviour and also of the *interactions between them*. A screening experiment should be thought of as a first step, giving a low-resolution but wide view, and should be followed by more specific and deeper experimental studies to give high-resolution views of the areas of behaviour which are seen to be important.

3. Experimental details

A 1 m^2, five-ply panel was laminated by hand using polyester resin reinforced with 500 gm^{-2} E-Glass balanced woven roving at a fibre mass-fraction of 50%. 0.5, 1 and 1.5% by mass of accelerator, catalyst and paraffin respectively were used to cure the resin. After curing, the panel was cut into specimens using a circular saw with a diamond-surrounded blade. Twenty-four 150 mm×100 mm specimens for use with the rectangular clamp, and twenty-four 100 mm×100 mm specimens for use with the circular clamp were produced. Four thickness measurements were then taken from each specimen.

The impact tests were carried out using a Rosand IFW5 instrumented drop-weight tower. A striker is dropped from a known, variable height, and hence at a known incident velocity, onto a horizontally supported plate target. The specimen is clamped between steel plates by a pneumatically operated lever arm providing a high clamping force. A variable mass attached to the striker allows variation of the velocity at a given incident energy (or vice versa). A load cell between the striker and this mass allows measurement of the impact force, and an optical gate initiates the data acquisition and accurately records the incident velocity. This force–time data enables calculation by the software of the deflection and velocity of the striker (and hence of the centre of the specimen) and also of the energy absorbed by the specimen.

Since in this study the effect of impact velocity was not to be investigated, the two incident energy levels were achieved by dropping the same mass of 10.853 kg from different heights. The energy levels were selected using previous work as a guideline [18], the low '–' level set

at 20J and the high ‘+’ level at 80J. The rectangular and circular clamp geometries are shown in Fig. 2.

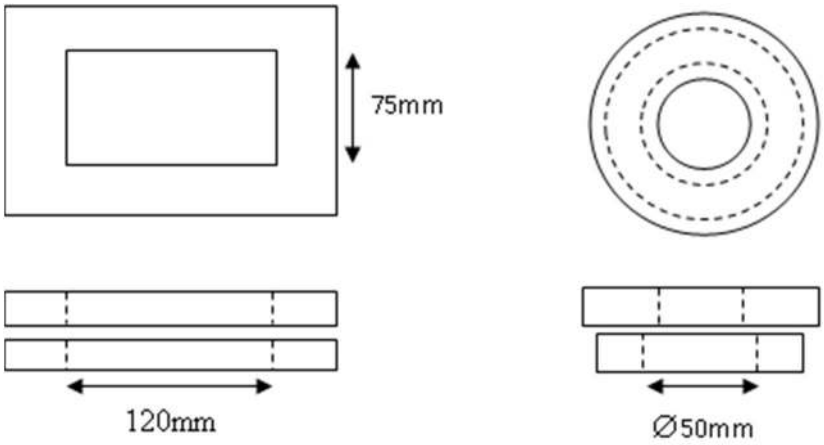

Fig. 2. Rectangular and circular clamps.

The circular clamp was arbitrarily assigned to the ‘–’ level and the rectangular to the ‘+’. Coarse sandpaper bonded onto the faces of the clamps was used to give the ‘Grip’ factor ‘+’ level. The strikers used were two 20 mm diameter stainless steel cylinders, one flat ended and one hemispherical. The factor levels were arbitrarily assigned as flat for ‘–’ and hemispherical for ‘+’. The factor levels are summarised in Table 2.

Factor / Level	**‘-’**	**‘+’**
Incident Energy ‘E’	20J	70J
Clamp ‘C’	Circular	Rectangular
Grip ‘G’	None	Sandpaper
Striker Head ‘H’	Flat	Hemispherical

Table 2. Factor levels

After the impact tests the specimens were photographed and the damage seen qualitatively described and recorded. Strong back lighting was then used to view any delamination, and the projected delaminated area measured.

4. Results

The experimental results are presented in Table 3, with the failure mode codes used defined in Table 4. It must be noted here that varying degrees of many subtly different failure modes were seen, but common features were distinguishable. The coding of failure modes was an attempt to categories these failure modes, and hence specimens with the same failure mode code suffered similar, but not necessarily identical damage. The main features of the failure modes are now described for the front face, internal delamination and back face damages. To simplify the descriptions, specimens may be referred to as ‘circular’ and ‘rectangular’ when clamped by the circular and rectangular frames respectively. Similarly those impacted using the flat and hemispherical impactors may be referred to as ‘flat-impacted’ and ‘hemisphere-impacted’ respectively.

4.1. Front face damage

For all specimens the warp of the reinforcement runs from side to side in the following photographs and figures. The main feature of the front face damage was delamination due to compression at ‘cross-over’ points where one roving passed over another, forming a pattern of small, elongated delaminated areas. In the central area of all specimens this occurred at both warp and weft ‘cross-overs’. However, at the edges of the damaged area, these delaminations were seen only where the warp crossed over the weft on rectangular specimens, and conversely only where the weft crossed over the warp on the circular specimens.

These delaminations formed a ‘butterfly' shape on the rectangular specimens (Fig. 3). For all of the rectangular specimens tested at the higher energy, and for two out of three of the rectangular hemisphere-impacted specimens tested at the lower energy, a shear crack formed at roughly 45° through the specimen, extending between the centre and the edge of the clamp (Fig. 4).

The surface delaminations formed a cross on the circular specimens (Fig. 5). For the higher energy perforation of the hemisphere-impacted specimens occurred (Fig. 6), and for the flat-impacted specimens the surface delaminations formed a diamond shape and a shear crack occurred (Fig. 7).

The flat impactor head gave a flat circular depression with some cut fibres at the edges for the higher impact energy and concentric circular resin cracks for all high energy impacts and approximately half of the low energy impacts. These circular resin cracks were also seen for all hemisphere-impacted specimens, where smaller, but deeper indentations were produced.

4.2. Internal delaminations

Here it should be noted that the method of viewing the internal damage using strong back-lighting did not allow the distinction between multiple delaminations at different positions through the thickness, only a projected shape of all damage was seen. However, with some care it was possible to distinguish between the internal delaminations and the front and back face damage.

For rectangular specimens impacted with the hemispherical head this delamination formed a small circle under the impactor (Fig. 8, Code 1). ‘Arms’ extended from this delamination for those rectangular specimens tested at the higher energy and also for those where no grip was used (Fig. 8, Code 2). For all rectangular flat-impacted specimens two small ‘lugs’ were formed either side of the impactor at the lower impact energy (Fig. 8, Code 3). At higher energies a central ring with arms was seen (Fig. 8, Code 4), with these arms bending slightly towards the shear crack to form an open ‘C'shape when no grip was used.

Circular hemisphere-impacted specimens suffered a circular delamination up to the clamp edge (Fig. 9, Code 5). Circular flat-impacted specimens suffered an annular delamination from the edge of the head to the clamp edge (Fig. 9, Code 6). No effect of grip on the damage shape was seen for this clamp geometry, but at the higher energy the delamination extended slightly beyond the clamp edge.

	Thickness (mm)					Coded Factors				Max. Force	Max. Defln.	Absorbed Energy	Damage Area	Failure Modes		
Code	t1	t2	t3	t4	t ave	Energy	Head	Grip	Clamp	(kN)	(mm)	(J)	(dm^2)	Front Face	Internal Delam.	Back Face
HC/A1	3,41	2,79	2,61	3,12	2,98	-1	1	-1	1	3,53	8,722	18,94	0,390	2	1	2
HC/B1	3,12	3,11	2,89	3,03	3,04	-1	1	-1	1	3,70	8,203	18,90	0,366	2	1	2
HC/C1	3,64	3,11	2,85	3,22	3,21	-1	1	-1	1	3,88	7,982	17,35	0,374	1	1	2
HC/A3	3,15	2,97	3,10	3,04	3,07	-1	-1	-1	1	4,50	7,034	19,96	0,303	2	3	1
HC/B3	3,09	3,19	3,46	3,61	3,34	-1	-1	-1	1	4,81	6,785	16,41	0,275	1	3	1
HC/C3	3,41	3,29	3,30	3,70	3,43	-1	-1	-1	1	4,74	6,784	16,17	0,386	1	3	1
HC/A5	3,18	2,97	2,81	3,12	3,02	-1	1	1	1	4,27	7,712	18,26	0,204	1	1	2
HC/B5	3,22	3,11	3,09	3,15	3,14	-1	1	1	1	4,71	7,207	17,07	0,220	1	1	2
HC/C5	3,42	3,36	3,12	3,43	3,33	-1	1	1	1	4,35	7,461	16,89	0,240	1	1	2
HC/A7	3,17	2,94	2,97	3,10	3,05	-1	-1	1	1	4,97	6,652	16,72	0,350	1	3	1
HC/B7	3,34	3,23	3,38	3,37	3,33	-1	-1	1	1	4,96	6,415	15,74	0,313	1	3	1
HC/C7	3,25	3,31	3,23	3,20	3,25	-1	-1	1	1	4,88	6,659	16,00	0,315	1	3	1
HC/D3	3,30	3,08	3,15	3,24	3,19	-1	1	-1	-1	6,42	5,893	19,99	0,217	3	5	3
HC/E3	3,52	3,45	3,47	3,50	3,49	-1	1	-1	-1	6,72	5,746	19,27	0,217	3	5	3
HC/F3	3,38	3,51	3,41	3,38	3,42	-1	1	-1	-1	6,80	5,805	19,17	0,200	3	5	3
HC/D1	3,35	3,25	2,82	2,92	3,09	-1	-1	-1	-1	8,78	4,353	17,15	0,270	3	6	1
HC/E1	3,34	3,63	3,06	3,35	3,35	-1	-1	-1	-1	9,09	4,286	17,89	0,273	3	6	1
HC/F1	3,34	3,19	3,02	3,47	3,26	-1	-1	-1	-1	8,82	4,363	18,00	0,283	3	6	1
HC/D5	3,37	3,12	3,37	3,45	3,33	-1	1	1	-1	6,50	5,738	18,94	0,295	3	5	3
HC/E5	3,37	3,66	3,48	3,61	3,53	-1	1	1	-1	6,59	5,482	17,80	0,280	3	5	3
HC/F5	3,34	3,62	3,41	3,44	3,45	-1	1	1	-1	6,63	5,800	19,75	0,210	3	5	3
HC/D7	3,28	3,29	3,19	3,34	3,28	-1	-1	1	-1	8,72	4,312	16,47	0,261	3	6	1
HC/E7	3,49	3,31	3,44	3,36	3,40	-1	-1	1	-1	9,07	4,030	16,46	0,247	3	6	1
HC/F7	3,42	3,38	3,47	3,51	3,45	-1	-1	1	-1	8,95	4,083	16,62	0,287	3	6	1
HC/A2	3,35	2,92	2,87	3,11	3,06	1	1	-1	1	5,01	20,360	78,32	0,735	2	2	3
HC/B2	3,24	3,05	3,13	3,38	3,20	1	1	-1	1	4,93	20,106	76,71	0,700	2	2	3
HC/C2	3,46	3,29	3,35	3,38	3,37	1	1	-1	1	5,01	20,602	77,39	0,810	2	2	3
HC/A4	3,37	2,88	2,88	3,03	3,04	1	-1	-1	1	5,56	18,663	76,18	0,926	2	4	1
HC/B4	3,29	2,96	3,09	3,35	3,17	1	-1	-1	1	5,97	16,377	70,66	0,879	2	4	1
HC/C4	3,28	3,26	3,25	3,43	3,31	1	-1	-1	1	3,19	15,823	70,36	0,829	2	4	1
HC/A6	3,21	2,94	3,04	3,47	3,17	1	1	1	1	5,43	18,571	75,34	0,742	2	2	3
HC/B6	3,24	3,38	3,10	3,55	3,32	1	1	1	1	5,91	17,305	74,54	0,656	2	2	3
HC/C6	3,23	3,24	3,39	3,24	3,28	1	1	1	1	6,34	17,151	74,80	0,685	2	2	3
HC/A8	3,76	3,30	2,99	3,20	3,31	1	-1	1	1	6,80	14,912	70,87	0,788	2	4	1
HC/B8	3,48	3,65	3,45	3,23	3,45	1	-1	1	1	7,18	14,147	70,55	0,896	2	4	1
HC/C8	3,56	3,72	3,34	3,36	3,50	1	-1	1	1	7,56	14,185	70,15	0,780	2	4	1
HC/D4	3,23	3,28	3,21	3,32	3,26	1	1	-1	-1	8,63	-	78,22	0,390	4	5	4
HC/E4	3,27	3,47	3,38	3,46	3,40	1	1	-1	-1	8,65	-	78,84	0,285	4	5	4
HC/F4	3,33	3,36	3,32	3,70	3,43	1	1	-1	-1	8,85	-	78,14	0,286	4	5	4
HC/D2	3,42	3,29	3,44	3,77	3,48	1	-1	-1	-1	16,15	8,066	67,59	0,451	5	6	2
HC/E2	3,51	3,55	4,25	3,42	3,68	1	-1	-1	-1	17,14	7,813	68,39	0,494	5	6	2
HC/F2	3,44	3,49	3,43	3,42	3,45	1	-1	-1	-1	18,33	7,750	69,02	0,514	5	6	2
HC/D6	3,33	3,36	3,43	3,36	3,37	1	1	1	-1	8,57	-	78,23	0,295	4	5	4
HC/E6	3,42	3,47	3,50	3,41	3,45	1	1	1	-1	8,60	-	78,28	0,265	4	5	4
HC/F6	3,43	3,40	3,27	3,37	3,37	1	1	1	-1	8,53	-	78,40	0,262	4	5	4
HC/D8	3,39	3,34	3,26	3,26	3,31	1	-1	1	-1	18,26	7,658	67,66	0,482	5	6	2
HC/E8	3,42	3,52	3,42	3,40	3,44	1	-1	1	-1	18,05	7,931	65,56	0,434	5	6	2
HC/F8	3,58	3,38	3,35	3,62	3,48	1	-1	1	-1	18,90	7,634	63,67	0,420	5	6	2

Table 3. Experimental results

Front Face	**Internal Delamination**	**Back Face**
1 Rectangle / Butterfly	1 Central Circle	1 Matrix Cracks
2 Butterfly + Shear Crack	2 Central Circle + Arms	2 Matrix Cracks + Slight Fibre / Matrix Damage
3 Cross / Diamond	3 Lugs	3 Matrix Cracks + Fibre / Matrix Damage
4 Cross / Diamond + Perforation	4 Central Ring + Arms	4 Matrix Cracks + Perforation
5 Cross / Diamond + Shear Crack	5 Circle to Clamp Edge	
	6 Ring to Clamp Edge	

Table 4. Failure mode codes

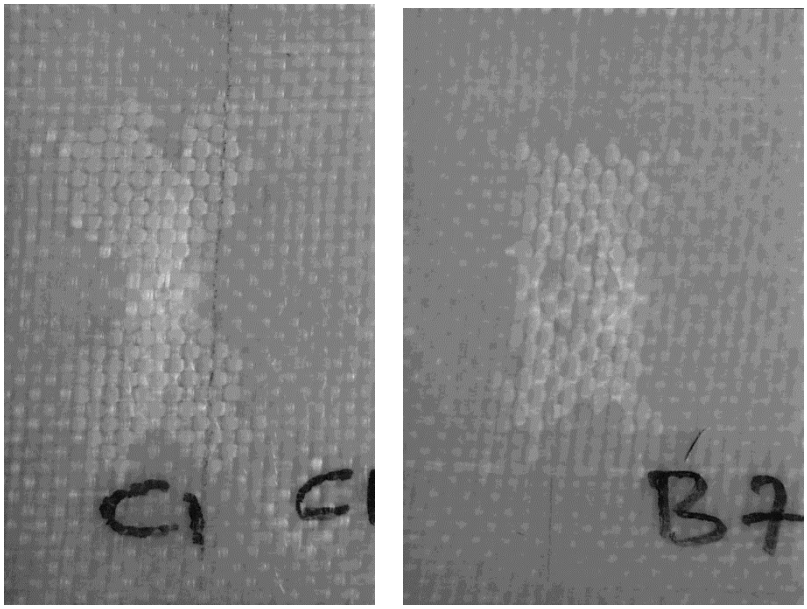

Fig. 3. Front face code 1: butterfly delamination.

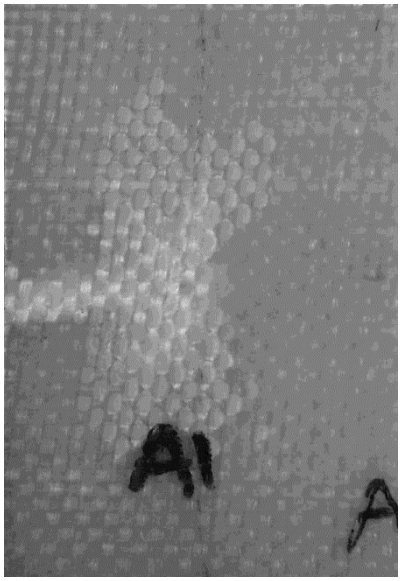

Fig. 4. Front face code 2: butterfly delamination with shear cracks.

Fig. 5. Front face code 3: cross delamination.

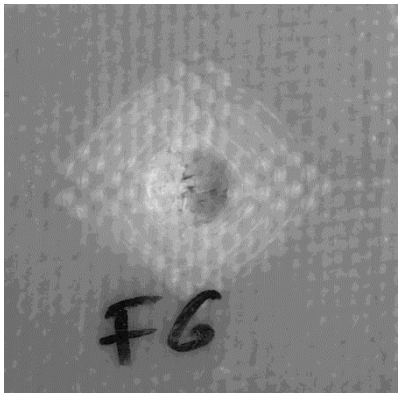

Fig. 6. Front face code 4: cross delamination with perforation.

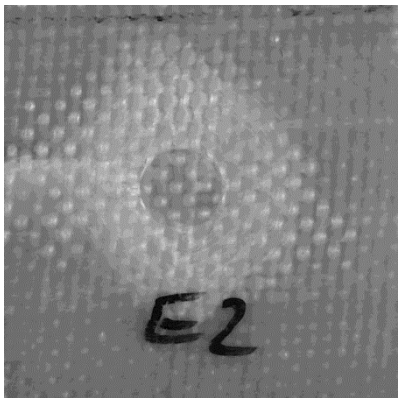

Fig. 7. Front face code 5: cross delamination with shear crack.

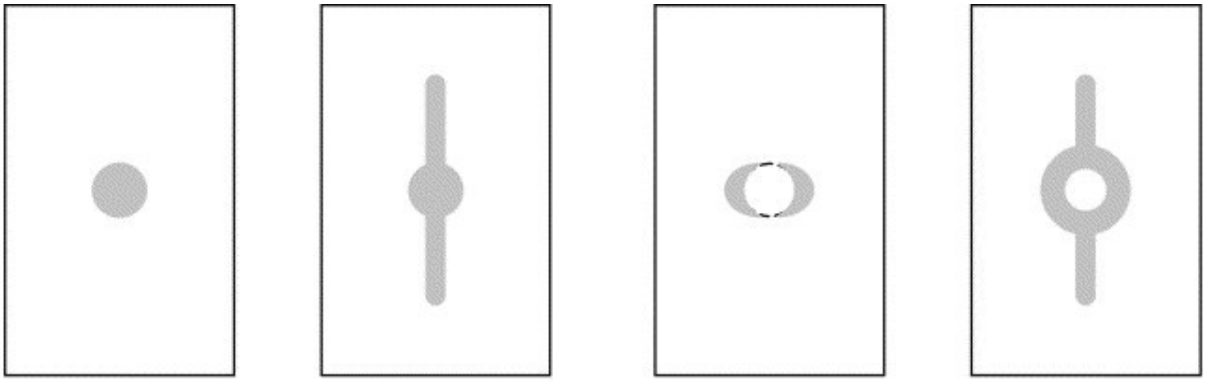

Fig. 8. Rectangular clamp internal delaminations.

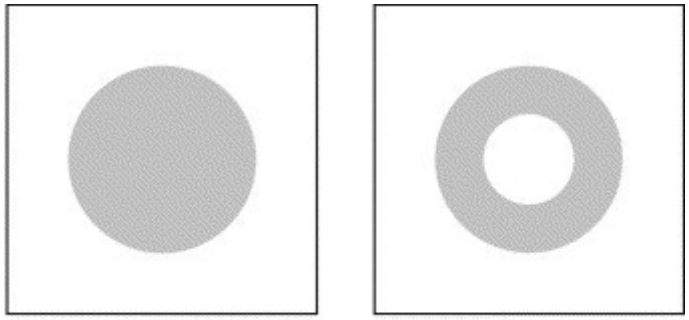

Delamination Code 5: Circle to Clamp Edge

Delamination Code 6: Ring to Clamp Edge

Fig. 9. Circular clamp internal delaminations.

4.3. Back face damage

A feature of all specimens was the cracking of the matrix on the back face. These cracks generally followed the woven rovings but also, especially for the higher impact energy, others extended radially from the centre (Fig. 10). The shape of the area of matrix cracking approximately followed that of the front face damage.

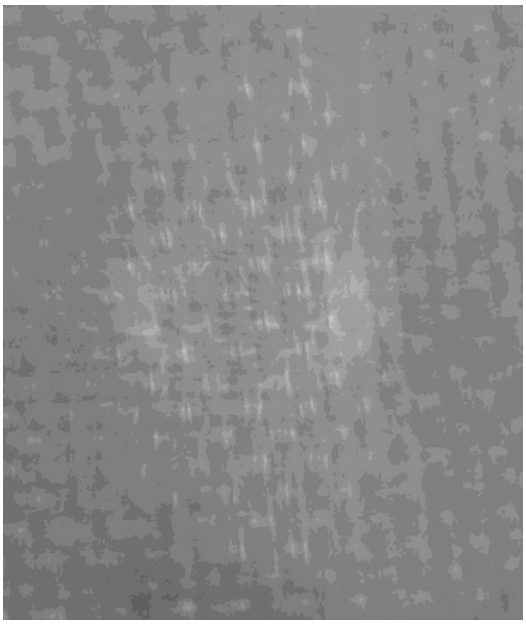

Fig. 10. Back face code 1: matrix cracks.

At the higher impact energy matrix destruction and fibre damage at the centre of the back face also occurred. For the lower impact energy slight matrix and fibre damage occurred on the hemisphere-impacted specimens only (Fig. 11). This damage was more severe for the circular specimens (Fig. 12). High-energy impact of the circular specimens with the hemispherical impactor gave almost complete penetration, with severe back face damage in a raised ‘dome’ (Fig. 13). At the higher impact energy deformation of the specimen at the clamp edge gave rise to compression roving ‘cross-over’ delaminations as seen on the front face, especially on the circular specimens.

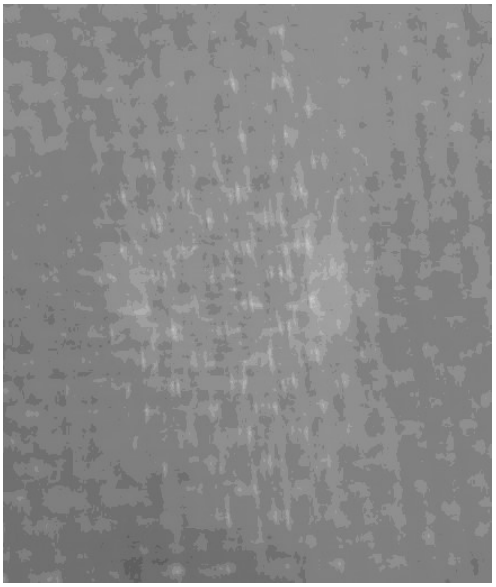

Fig. 11. Back face code 2: matrix cracks with slight fibre and matrix damage.

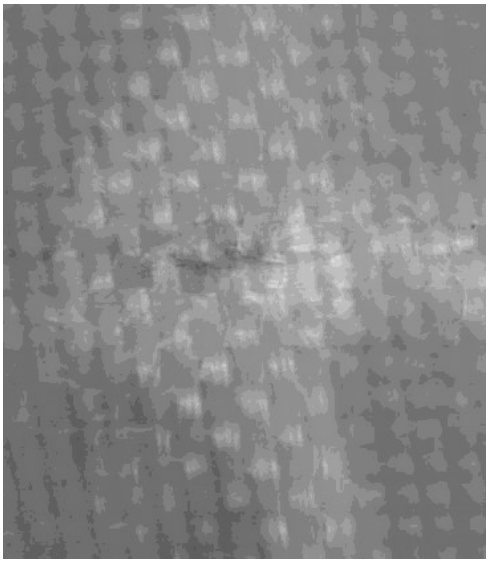

Fig. 12. Back face code 3: matrix cracks with fibre and matrix damage.

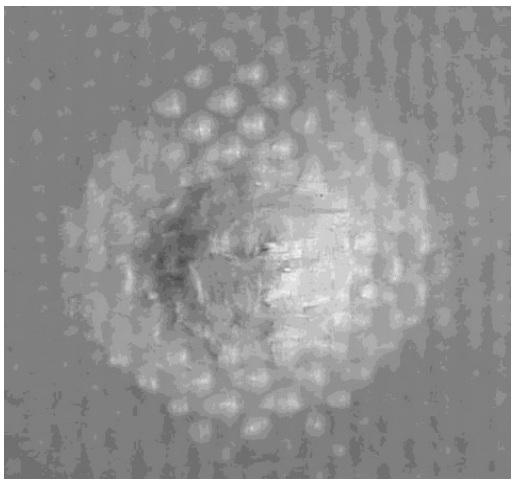

Fig. 13. Back face code 4: matrix cracks with perforation.

5. Analysis of results

5.1. Graphical presentation and statistical analyses

An initial attempt was made to statistically analyse the full data set as a whole to give the four factor effects and their interactions. However, a residual analysis (see Section 2.4) showed that the experimental variability differed between the low and high impact energy levels. Since experimental variability that is constant across the factor levels is a basic assumption of the statistical methods used, the data and the analysis were split into two parts, corresponding to the low and high incident energy levels. This decision also makes the graphical representation of the results that follows much simpler.

The results will be presented as a series of two-way interaction plots between the factors 'Grip' and 'Head'. The low and high-energy results are plotted in Figs. 14 and 15 respectively. A graph for the square clamp and the corresponding one for the circular clamp are given for each of the three responses maximum force, irreversibly absorbed energy and damage area. This enables the interpretation of any three-way interaction 'H×G×C' by comparing the two 'G×H' interaction graphs for the required response.

The variation of the different failure modes seen between factor levels will help to explain some of the effects seen and so these are represented in a similar manner in Figs. 16 and 17 for the low and high energy results respectively. The coded values used in these plots are as defined inSection 4. Again it must be noted that specimens with the same failure mode code suffered similar, but not necessarily identical damage.

An ANOVA approach (see Section 2.4) was used to fit a full three-way interaction statistical model to the data for each response in turn. Coded values of −1 and +1 were used for the '–' and '+' factor levels respectively. Since specimen thickness, *t*, was seen to have considerable variation and is known to affect the impact responses, this term was also included in the model as a co-variate. In some cases the specimen was completely perforated and hence the data set for the maximum deflection response was not complete. A restriction of the statistical method used is that all of the data must be available in order that the experimental design retains its balance and so the analysis of this response was not possible. Hence, the responses analysed were maximum force, absorbed energy and damaged area.

The statistical model used throughout was:

$$y = C + G + H + CxG + CxH + GxH + CxGxH + t + \varepsilon \qquad (3)$$

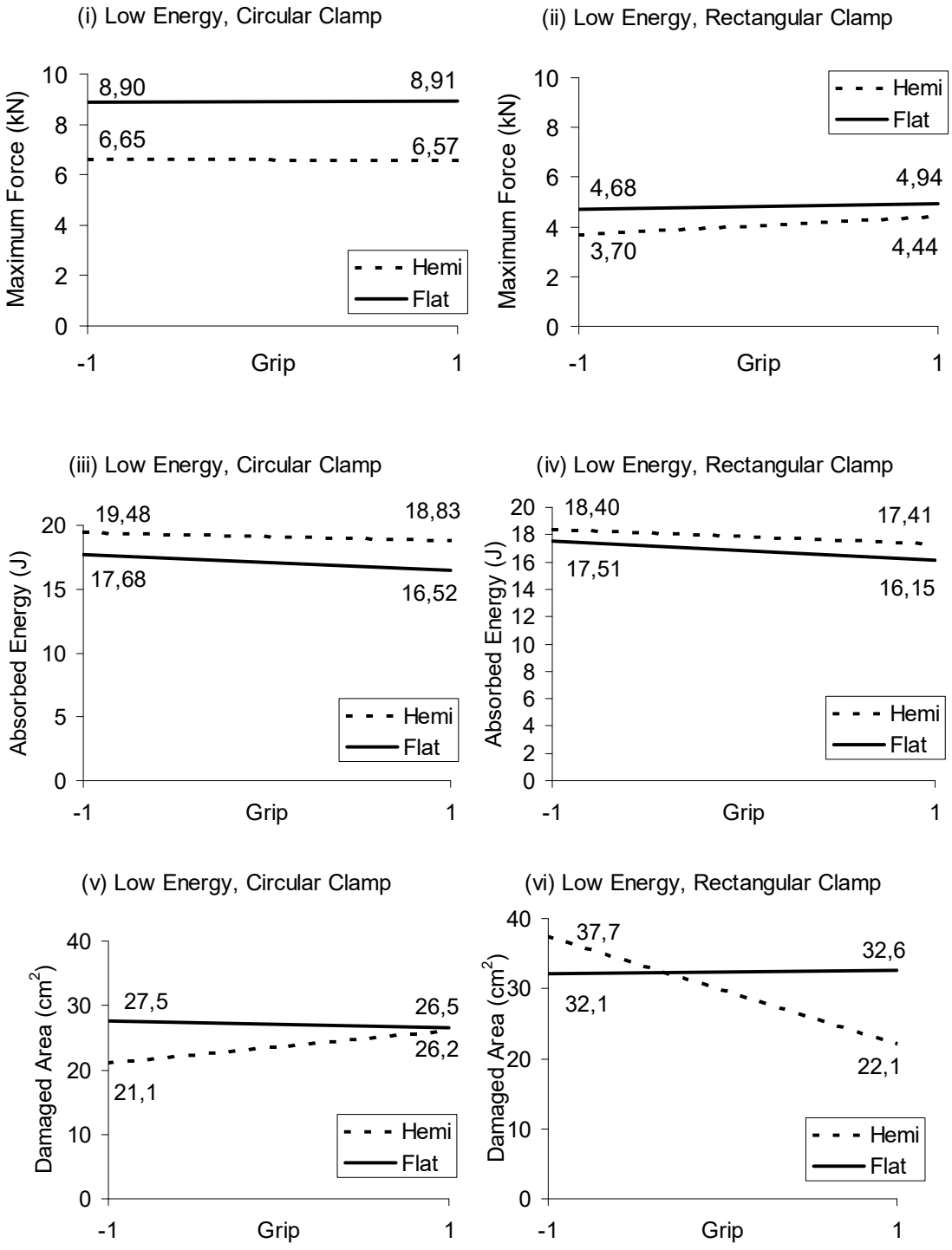

Fig. 14. Low energy factor interaction plots.

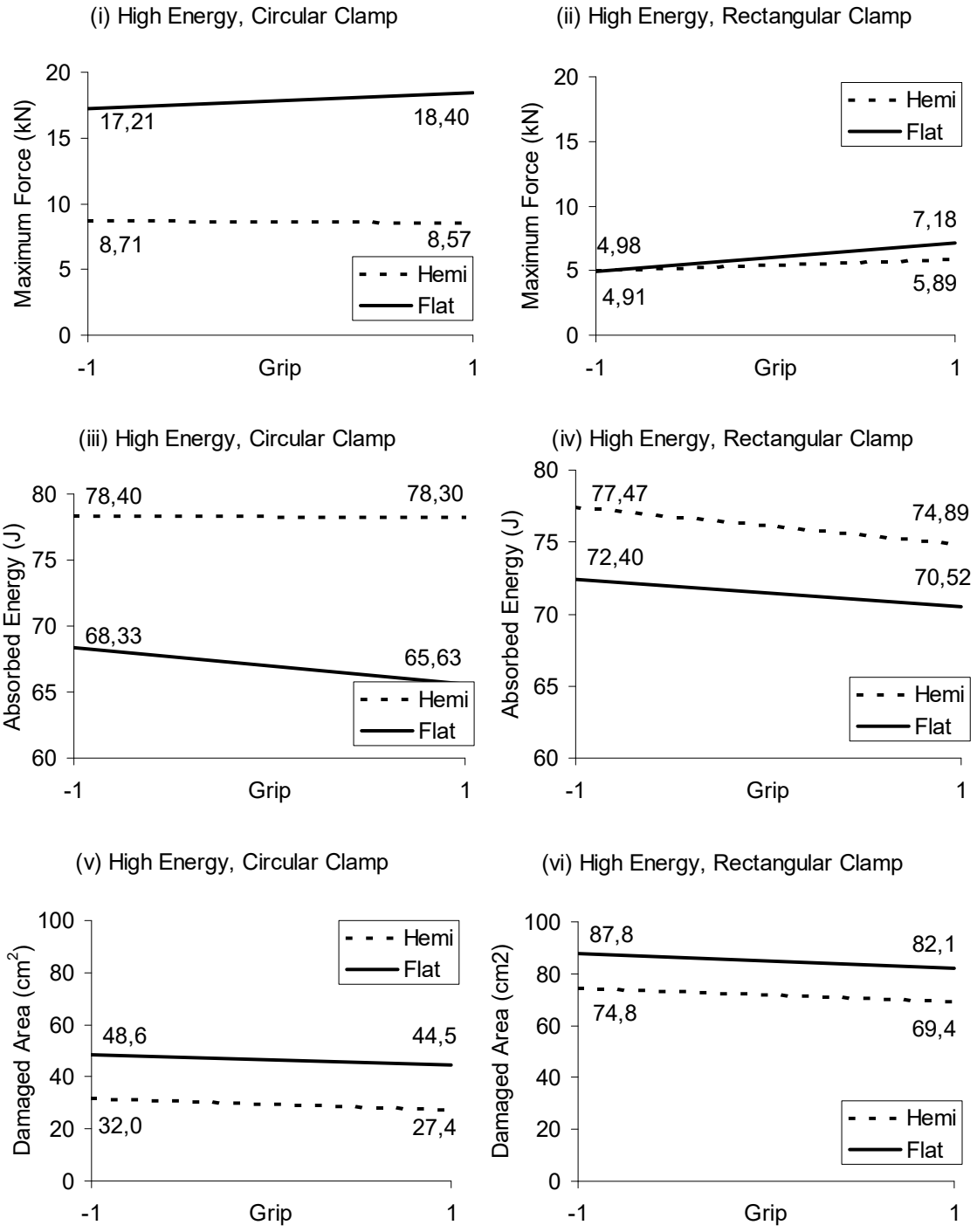

Fig. 15. High energy factor interaction plots.

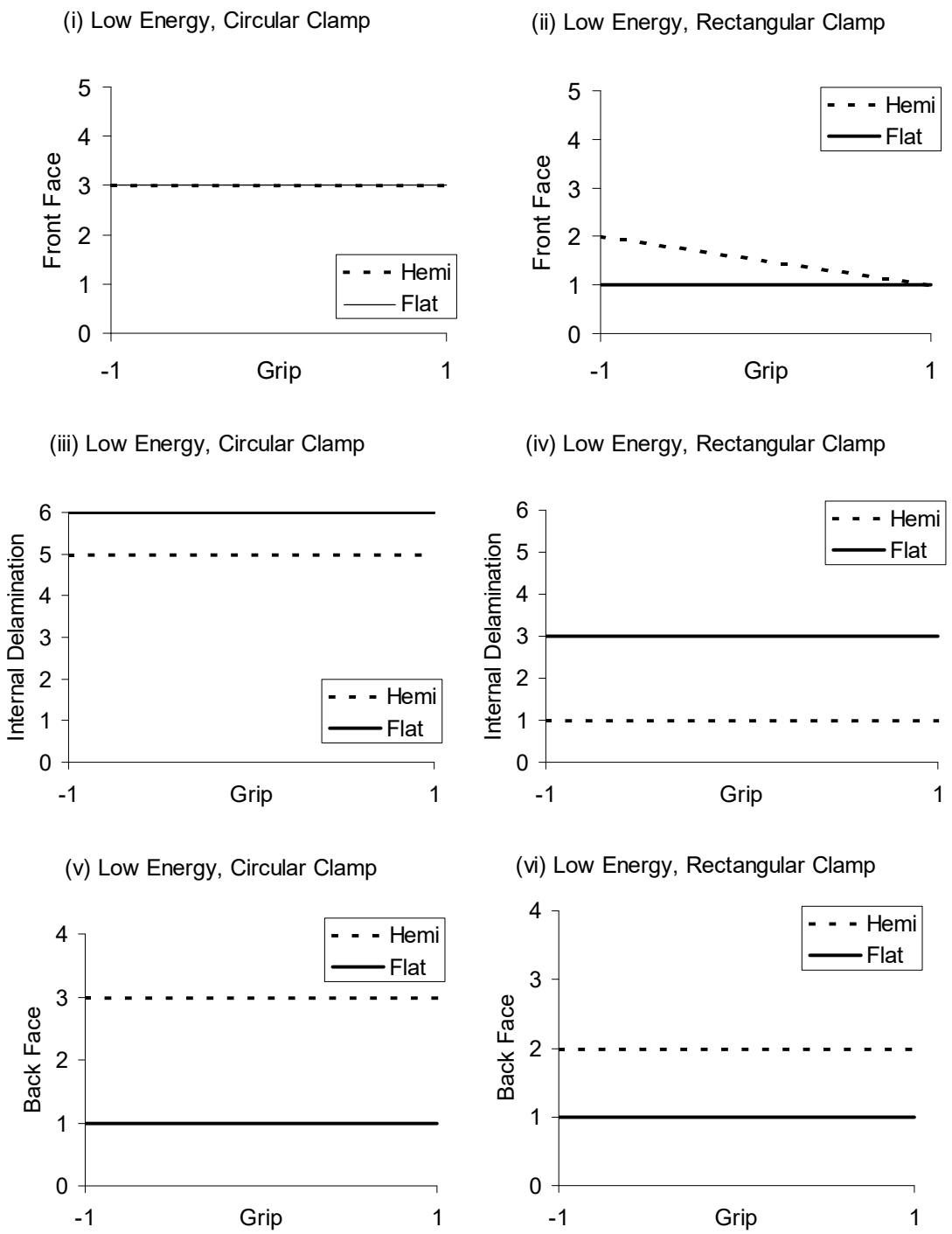

Fig. 16. Low energy failure mode plots.

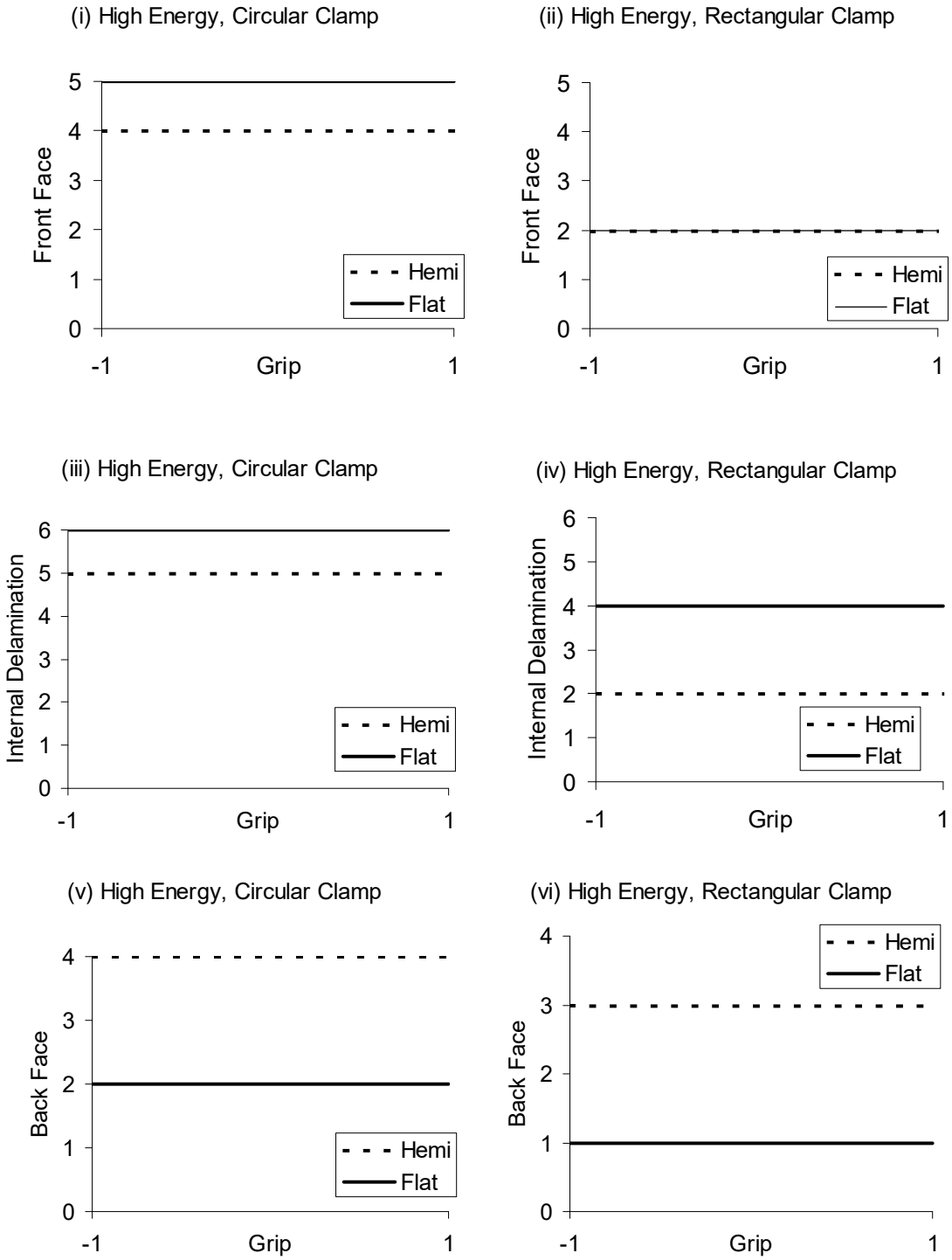

Fig. 17. High energy failure mode plots.

In these cases the residual analyses did not show any need for concern. In order to obtain the *R*-squared values the analyses were also carried out using the Multiple Linear Regression method (see Section 2.4). Summaries of the results of these analyses are given in Tables 5 and 6. *P*-values that are statistically significant at a 5% level are in shown in bold type. For the reasons outlined in Section 2.3, it should be noted that apparently non-significant main effects with significant interaction effects and apparently non-significant two-way effects that are a subset of significant three-way interaction effects may also be important.

Term	Maximum Force		Absorbed Energy		Damaged Area	
	Coefficient	p-value	Coefficient	p-value	Coefficient	p-value
Head	-0.75280	**0.000**	0.7476	**0.000**	-0.014397	**0.033**
Grip	0.09632	**0.004**	-0.3852	**0.026**	-0.014591	**0.036**
Clamp	-1.59624	**0.000**	-0.7795	**0.001**	0.031252	**0.001**
HxG	0.04206	0.152	0.1597	0.310	-0.12691	0.057
HxC	0.42960	**0.000**	-0.5064	**0.009**	0.003711	0.594
GxC	0.14900	**0.000**	-0.1827	0.257	-0.023185	**0.002**
HxGxC	0.05132	0.093	0.1164	0.468	-0.028341	**0.000**
Thickness	0.7220	**0.010**	-4.687	**0.003**	0.02636	0.632
R^2 (adj.)	99.5%		69.5%		73.9%	

Table 5. Low energy level statistical analyses results

Term	Maximum Force		Absorbed Energy		Damaged Area	
	Coefficient	p-value	Coefficient	p-value	Coefficient	p-value
Head	-2.4836	**0.000**	3.7299	**0.000**	-0.7883	**0.000**
Grip	0.5556	**0.002**	-0.7200	**0.014**	-0.021827	**0.044**
Clamp	-3.8244	**0.000**	-0.0269	0.938	0.19255	**0.000**
HxG	-0.3431	**0.035**	0.2005	0.435	-0.000918	0.925
HxC	2.1482	**0.000**	-1.6060	**0.000**	0.010960	0.271
GxC	0.3165	0.080	0.1545	0.595	0.00273	0.806
HxGxC	-0.0497	0.769	-0.7504	**0.017**	-0.00426	0.697
Thickness	-1.039	0.546	-7.482	**0.019**	-0.1169	0.301
R^2 (adj.)	98.0%		93.4%		95.7%	

Table 6. High energy level statistical analyses results

5.2. Interpretation of statistical analyses

The fit of the statistical model to the data was very good for the maximum impact force at both low and high energy levels (R^2 values of 99.5 and 98.0% respectively), and for irreversibly absorbed energy and projected damage area at the higher impact energy level (R^2 values of 93.4 and 95.7%, respectively). At the low energy level the fit of the statistical models to the data for absorbed energy and damage area were lower (R^2 values of 69.5 and 73.9%), but still indicating a reasonably good fit to the data.

The results of the statistical analyses show that the impact behaviour is complex, with many interactions between the factors studied. The 'statistically significant' (i.e. distinguishable) effects and their trends have been identified through cross-referencing between the statistical and graphical data in Section 5.1. The significant effects were identified from Tables 5 and 6 and then the natures of these obtained from Figs. 14 and 15 respectively.

The variable specimen thickness, *t*, was found to have a significant effect on the impact responses. The effects of each of the parameters [impactor head (*H*), the use of grip on the clamp faces (*G*), and the clamp shape (*C*)] were significantly large for all three measured system responses [maximum impact force (*F*), absorbed energy (*AE*) and projected damaged area (*DA*)] at both high and low impact energies, with the exception of the effect of the clamp geometry on the absorbed energy at the high impact energy level. These factor main effects were similar at both energy levels. Interactions between these parameters and with the impact energy were also found to be important.

The findings are summarised below and may used with reference to the relevant significant *P*-values (in bold) in Table 5 and 6 and the effects plots of Figs. 14 and 15. Each significant effect is represented as a function of its response, for example the effect of thickness on the maximum force is represented as *t*(*F*). Physical interpretations of the behaviour seen have been postulated, using the failure mode plots of Figs. 16 and 17 for guidance.

(i) *t*(*F,AE*): The higher maximum forces measured for the thicker specimens at the low impact energy were not seen for the higher energy. Thicker specimens irreversibly absorbed less energy. A thicker specimen is stiffer and will thus exert higher forces on the impactor at lower bending/shear strains leading to higher local damage but lower structural damage. It appears that in this case the latter damage is dominant.

(ii) *H*(*F*,*AE*,*DA*): On average, the hemispherical head, when compared to the flat head, gave lower maximum forces, higher absorbed energies and lower damage areas. The differences here are due to the different damage and failure modes produced by the each impactor head. Due to the smaller contact area and hence higher contact and through-thickness stresses, the hemispherical impactor gave more indentation on the front face and in general more back face matrix and fibre damage leading to perforation.

(iii) *G*(*F*,*AE*,*DA*): On average, the use of coarse sandpaper grip on the clamp faces, as opposed to using the bare metal faces, gave higher maximum forces, lower absorbed energies and lower damage areas. This shows that without the grip, some degree of slippage between the clamps was occurring. Reducing this slippage would increase the plate stiffness due to increased in-plane stresses and thus reduce bending/shear strains. The inclusion of grip has prevented the shear-crack failure of the hemisphere-impacted rectangular specimens as seen in Fig. 16 (ii).

(iv) *C*(*F*,*AE*,*DA*): On average, the use of the rectangular clamp, when compared to that of the circular clamp, gave lower maximum forces, lower absorbed energies and higher damage areas. For the high impact energy the effect of the clamp on the absorbed energy, although present, was weaker. The smaller, and hence stiffer circular specimens produce higher contact forces and through thickness stresses, leading to more severe damage and greater absorbed energy. The plots (iii) of Figs. 16 and 17 show that the internal delaminations were restricted by the circular clamp, giving lower damaged areas for the circular specimens.

(v) *G*×*H*(*F*): At the higher impact energy the increasing effect of grip on the maximum force was greater for the flat head than for the hemispherical head. At the lower impact energy this interaction between head shape and the use of grip was not seen. The higher forces exerted by the flat head [see (ii) above] would lead to greater slippage and hence a greater effect of the use of grip.

(vi) *H*×*C*(*F*,*AE*): At both impact energy levels the effects of head shape on maximum force (higher *F* with flat impactor head) and absorbed energy (lower *AE* with flat impactor head) were greater for the circular clamp than for the rectangular clamp. Since the smaller, stiffer circular specimens suffered higher contact forces and more severe damage [see (iv) above], the effects of head shape attributed to the different damage modes seen [see (ii) above] would be more marked for the circular clamp.

(vii) *G*×*C*(*F*): At the low impact energy the increase in maximum force due to the use of grip for the rectangular clamp was not seen for the circular clamp. A similar, but weaker effect was present at the high impact energy. This effect is mainly due to the prevention of the shear-crack in the hemisphere-impacted rectangular specimens by the use of grip [see (ii) above]. The larger deflections of the larger rectangular specimens led to greater in-plane stresses, more possibility of slippage and hence a greater effect of the use of grip.

(viii) *H*×*G*×*C*(*AE*): At the high impact energy using grip reduced the absorbed energy for both impactor heads with the rectangular clamp, but only for the flat impactor head when the circular clamp was used. At the lower impact energy this three-way interaction was not seen. It is only at the high impact energy for the hemisphere-impacted circular specimens that perforation occurs [see Fig. 17 (i) and (v)]. The lower forces and plate deflections associated with this failure mode would reduce the influence of the use of grip.

(ix) *H*×*G*×*C*(*DA*) and *G*×*C*(*DA*): The following behaviour was seen only at the low impact energy. For both clamp geometries there was little change in damage area with the inclusion of grip for the flat impactor head. However, for the hemispherical head the introduction of grip increased the damage area for the circular clamp whereas it decreased the damage area for the rectangular clamp. The large reduction in damage area due to the prevention of the shear-crack failure of the hemisphere-impacted rectangular specimens by the use of grip [see (ii) above] drives this effect.

It should be noted that the damage area values are often projections of multiple delaminations and so care should be taken in interpreting these results. Also, delamination is not the only damage mode present, fibre breakage and matrix cracking and destruction also occur. This means that although damage area and absorbed energy are related, they do not necessarily follow the same trends and an increase in the severity of the damage does not always lead to an increase in the damaged area (e.g. point (ii) above where an increase in back face fibre and matrix damage gives a higher absorbed energy but a lower damage area).

6. Conclusions

The behaviour was complex, with specimen thickness, impactor shape and specimen geometry all influencing the impact response. The significant effect of the inclusion of grip on the faces of the clamps showed that, as suspected, slippage of the specimens between the smooth metal clamps occurred to some degree. Both the magnitude and the form of the effects of each parameter were in many cases dependant on the values taken by the other parameters. The different effects seen were often due to changes in the multiple damage mechanisms and failure modes occurring. Simple graphical representation of the different failure modes aided the interpretation of the data. Now that a global view of the system response has been shown, further experimentation is needed to investigate the important aspects in more detail.

Because of the complex and multiple failure modes present it is very difficult to quantify the damage incurred. The projected damage area has been used as a first approximation, but the interpretation of this is limited since it is only one of several types of damage, and may itself be made up of several distinct damage areas. Consideration of the energy irreversibly absorbed by the specimen gives a better indication of the total damage, but does not allow the different mechanisms to be distinguished.

Experimental design techniques have provided a simple and methodical approach to identifying the main features of this complex behaviour above the experimental variation. Some important points concerning the use of these techniques to explore this type of system follow from the results of this work:

- Simple graphical representations of the effects of the parameters on the measured responses, and on the failure modes seen, should be used *together with* the statistical analyses in order to physically interpret the data.
- Where there is thought to be interaction between many of the parameters simple experimental designs that use most or all of the combinations of parameter settings should be used. Also the number of parameters considered should be kept as small as possible to facilitate the graphical representation of the data.
- If the failure modes seen between distinct parts of the experiment are very different, then it may be necessary to split the statistical analyses into corresponding separate parts to satisfy the assumption of these analyses that the experimental variance is constant.
- The statistical analyses rely on the fact that a complete and consistent data set is available, which may place restrictions on the experimental process. The design (including the parameter settings) may not be revised during experimentation, and lost data due to unforeseen events may jeopardise or impair the successful analysis of the results.

Acknowledgements

The first author has been financed by Fundaçâo para a ciência e a Tecnologia, Lisbon, Portugal, under contract number SFRH/BPD/1568/2000.

References

1. Abrate S. Impact Damage on Composite Structures. Cambridge University Press, 1998.
2. Naik NK, Chandra Sekher Y and Sailendra Meduri. Damage in woven-fabric composites subjected to low-velocity impact. Composites Science and Technology 2000; 60: 731-744.
3. Kim JK and Sham ML. Impact and delamination failure of woven-fabric composites. Composites Science and Technology 2000; 60: 745-761.
4. Kim JK and Kang KW. An analysis of impact force in plain-weave glass/epoxy composite plates subjected to transverse impact. Composites Science and Technology 2000; 60: 135-143.
5. Mouritz AP, Gellert E, Burchill P and Challis K. Review of advanced composite structures for naval ships and submarines. Composite Structures 2001; 53: 21-41.

6. Richardson MOW and Wisheart MJ. Review of low-velocity impact properties of composite materials. Composites Part A 1996; 27A: 1123-1131
7. Sierakowski RL and Chaturvedi SK. Impact loading in filametary structural composites. Shock Vibration Digest 1983; 15(10): 13-31
8. Sjoblom P, Hwang B. Compression after impact: The $5000 data point. 34th Int SAMPE Symp Conference Proceedings, Reno 1989. p. 1411-1421.
9. Sun CT, Dicken A, Wu HF. Characterization of impact damage in ARALL laminates. Composite Science and Technology 1993; 49: 139-144.
10. Yang SH, Sun CT. Indentation law for composite laminates. ASTM STP 787 1982:425-449.
11. Chen JK, Sun CT. Dynamic large deflection response of composite laminate subject to impact. Composite Structures 1985; 4(1): 59-73.
12. Davies GAO, Zhang X. Impact damage prediction in carbon composite structures. Int J Impact Eng 1995; 16(1): 149-170.
13. Zhou G, Davies GAO. Impact response of thick glass fibre reinforced polyester laminates. Int J Impact Eng 1995; 16(3): 357-374.
14. Abrate S. Modeling of impacts on composite structures. Composite Structures 2001; 51: 129-138.
15. Graves MJ, Koontz JS. Initiation and extent of impact damage in graphite/epoxy and graphite/PEEK composites. 29th AIAA Struct Dyn Dyn Mat Conference Proceedings, Williamsburg 1988. p. 967-975.
16. Davies GAO, Zhang X, Zhou G, Watson S. Numerical modelling of impact damage. Composites 1994; 25(5): 342-350.
17. Frock BG, Moran TJ, Shimmin KD, Martin RW. Imaging of impact damage in composite materials. Rev Prog Quant Nondestr Eval 1988; 7(B): 1093-1099.
18. Sutherland LS, Guedes Soares C. Effects of laminate thickness and reinforcement type on the impact behaviour of E-glass/polyester laminates. Composites Science and Technology 1999; 59: 2243-2260.
19. Sutherland LS, Guedes Soares C. Impact tests on woven roving E-glass/polyester laminates. Composites Science and Technology 1999; 59: 1553-1567.
20. Gottesman T, Grishovich S, Drukka E, Sela N, Log J. Residual strength of impacted composites: analysis and tests, J Composites Tech and Research 1994; 16(3): 244-255.
21. Caprino G. Residual strength prediction of impacted composite laminates. J Composite Materials 1984; 18: 508-518.
22. Christoforou AP. Impact dynamics and damage in composite structures. Composite Structures 2001; 52: 181-188.
23. Caprino G, Lopresto V, Scarponi C and Briotti G. Influence of material thickness on the response of carbon-fabric/epoxy panels to low velocity impact. Composite Science and Technology 1999; 59: 2279-2286.
24. Caprino G and Lopresto V. On the penetration energy for fibre-reinforced plastics under low-velocity impact conditions. Composite Science and Technology 2001; 61: 65-73.
25. Cartié DDR and Irving PE. Effect of resin and fibre properties on impact and compression after impact performance of CFRP. Composites Part A 2002; 33: 483-493
26. Hirei Y, Hamada H and Kim JK. Impact response of woven glass-fabric composites – I. Effect of fibre surface treatment. Composite Science and Technology 1998; 58: 91-104.

27. Kessler A and Bledzki A. Correlation between interphase-relevant tests and the impact-damage resistance of glass/epoxy laminates with different fibre surface treatments. Composite Science and Technology 2000; 60: 125-130.
28. Morton J. Scaling of impact-loaded carbon fibre composites. AIIA J 1988; 26(8): 989-994.
29. Swanson SR. Interpretation of scaling of damage and failure in fiber composite laminates. ASC 8th Tech Conference Proceedings, 1993. p. 245-254.
30. Greenhalgh E, Bishop SM, Bray D, Hughes D, Lahiff S and Millson B. Characterisation of impact damage in skin-stringer composite structures. Composite Structures 1997; 36: 187-207.
31. Found MS, Howard IC and Paran AP. Impact behaviour of stiffened CFRP sections. Composite Structures 1998; 39(3-4): 229-235.
32. Found MS, Howard IC and Paran AP. Impact perforation of thin stiffened CFRP panels. Composite Structures 2000; 48: 95-98.
33. Fisher RA. Design of Experiments, 6th edn. Oliver & Boyd, 1951.
34. Taguchi G. Introduction to Quality Engineering. New York: Quality Resources, White Plains, 1986.
35. Grove DM, Davis PD. Engineering Quality & Experimental Design. Longman Scientific & Technical, 1992.
36. Mendenhall W, Sincich T. Statistics for Engineering and the Sciences. Prentice Hall, 1995.
37. Sutherland LS, Shenoi RA, Lewis SM. Size and scale effects in composites: I. Literature review. Composites Science and Technology 1998; 59: 209-220.
38. Sutherland LS, Shenoi RA, Lewis SM. Size and scale effects in composites: II. Unidirectional laminates. Composites Science and Technology 1998; 59: 221-233.
39. Sutherland LS, Shenoi RA, Lewis SM. Size and scale effects in composites: III. Woven-roving laminates. Composites Science and Technology 1998; 59: 235-251.
40. Sutherland LS. An investigation into composites size effects using statistically designed experiments. PhD Thesis, University of Southampton, Departments of Ship Science and Mathematics, 1997.